A Study of Nonlinearities and Intermodulation Characteristics of 3-Port Distributed Circulators

YOU-SUN WU, MEMBER, IEEE, WALTER H. KU, MEMBER, IEEE, AND JOHN E. ERICKSON

Abstract—**Results of a study of nonlinearities and intermodulation characteristics of 3-port distributed circulators are presented. Based on a rigorous theoretical analysis of the third-order nonlinearity in ferrites, analytical results are derived for the field strength and the power level of the intermodulation signal. These explicit results are applicable to high-power distributed circulators operating in VHF, UHF, and microwave frequencies. Measured intermodulation characteristics of an experimental distributed VHF high-power circulator are also presented.**

I. INTRODUCTION

IN THE small-signal approximation of ferrite behavior, higher order terms in magnetization and fields are neglected, thereby linearizing the equation of motion. However, for a number of practical applications the nonlinearities inherent in ferrites and large-signal effects become important. Examples of devices in which the ferrite nonlinearities are actually utilized include harmonic generators and mixers [1]–[4], ferrimagnetic amplifiers [4]–[7], and limiters [8]. More generally, large-signal and nonlinear effects are important considerations in almost all ferrite applications to ascertain the limitations on device characteristics for high-power operation.

This paper presents results on a study of nonlinearities and intermodulation characteristics of high-power circulators. Explicit results presented are for distributed 3-port or Y-junction circulators. Third-order nonlinearity of ferrites generates intermodulation noise in either lumped or distributed circulators. It is most severe in cases where collocated transmitting antennas are used. In these cases, it can seriously desensitize a receiver that is tuned to the frequency of any of the intermodulation products. The purpose of this paper is to give a complete theoretical study of the third-order nonlinearity of ferrites and its effects on circulators. The final goal is to derive some criteria for choosing ferrite materials such that a more "linear" circulator can be designed. These criteria will be useful for choosing material parameters to obtain better linearity characteristics without degrading other characteristics such as bandwidth and isolation.

In Section II, the third-order nonlinearities of ferrite are derived by an iterative procedure. This procedure gives accurate results without requiring an excessive amount of computation. In Section III, the coupling relationships between nonlinear third-order fields and magnetizations are derived. In Section IV, an illustrative example is presented for a specific VHF distributed 3-port circulator. The results derived using the theoretical analysis presented in this paper are compared to some experimental results actually measured on a high-power VHF isolator (Addington Laboratory).

II. NONLINEARITY AND INTERMODULATION NOISE IN FERRITES

Nonlinearity and large-signal effects of ferrites have been studied previously by Pippin [2], Jepsen [4], *et al.* mainly for the application of harmonic generation and frequency mixing. Their principal interest is in the second-order nonlinearities which produce the second harmonic and frequency mixing. In this paper, however, the third-order nonlinearity of ferrites is investigated and applied to calculate the dominant third-order intermodulation product in ferrites in 3-port circulators.

There are two types of nonlinearities. One arises under the assumption of uniform precession of the magnetization. The other is the nonuniform magnetization which causes the spin waves and has been studied previously by Suhl [8]. Since circulators are biased by a uniform magnetic field, this paper is confined to the study of nonlinearity which occurs under uniform precession.

The macroscopic theory of microwave ferrite devices is based on the equation of motion in terms of the magnetization vector $\boldsymbol{M}$. The well-known equation of motion [9] is given by

$$\frac{d\boldsymbol{M}}{dt} = \gamma \boldsymbol{M} \times \boldsymbol{H} \tag{1}$$

where

- $\boldsymbol{M}$ magnetization in gauss;
- $\boldsymbol{H}$ magnetic field inside the material in oersteds;
- γ $= 1.76 \times 10^7$ rad $(\text{s}\cdot\text{Oe})^{-1}$ is the gyromagnetic ratio;
- t time in seconds.

The total magnetic field in (1) consists of the dc magnetic bias field $\boldsymbol{H}_0$ and the magnetic field $\boldsymbol{h}$

Manuscript received March 26, 1975; revised July 14, 1975. This work was supported in part by the Federal Aviation Administration and the RADC Postdoctoral Program under U.S. Air Force Contract F30602-72-C-0497 and the work performed by W.H. Ku was supported by NSF Grant GK-31012X.

Y.-S. Wu was with the School of Electrical Engineering, Cornell University, Ithaca, NY 14850. He is now with the Central Research Laboratory, Texas Instruments Incorporated, Dallas, TX.

W. H. Ku is with the School of Electrical Engineering, Cornell University, Ithaca, NY 14850.

J. E. Erickson was with the Rome Air Development Center, Griffiss Air Force Base, NY 13441. He is now with the Department of Electrical Engineering, U.S. Air Force Academy, Colorado Springs, CO 80840.

$$\boldsymbol{H} = \boldsymbol{H}_0 + \boldsymbol{h}. \tag{2}$$

Similarly, the total magnetization is composed of the dc magnetization component $\boldsymbol{M}_0$ and the RF magnetization component $\boldsymbol{m}$

$$\boldsymbol{M} = \boldsymbol{M}_0 + \boldsymbol{m}. \tag{3}$$

Cylindrical coordinates are used here with the z-axis parallel to the direction of the dc magnetic field. Substituting (2) and (3) into (1) and expanding into the three field components result in the following fundamental relationships:

$$\frac{dm_r}{dt} = \gamma[m_\theta(H_0 - M_0 - m_z) - h_\theta(M_0 + m_z)] \tag{4}$$

$$\frac{dm_\theta}{dt} = \gamma[h_r(M_0 + m_z) - m_r(H_0 - M_0 - m_z)] \tag{5}$$

$$\frac{dm_z}{dt} = \gamma(m_r h_\theta - m_\theta h_r). \tag{6}$$

In the small-signal approximation, higher order terms of m and h in (4)–(6) are neglected and the preceding equations reduce to two simultaneous linear differential equations in m_r and m_θ (since (6) has no first-order terms). In this manner, the linearized theory of ferrites which is indicated by the Polder permeability tensor $\bar{\mu}$ is derived.

The Polder [10] permeability tensor $\bar{\mu}$ is given by

$$\bar{\mu} = \mu_0 \begin{bmatrix} \mu & j\kappa & 0 \\ -j\kappa & \mu & 0 \\ 0 & 0 & 1 \end{bmatrix} \tag{7}$$

where

$$\mu = 1 + \frac{\omega_0\omega_m}{\omega_0^2 - \omega^2}$$

$$\kappa = \frac{\omega\omega_m}{\omega_0^2 - \omega^2}$$

$$\mu_0 = 4\pi \times 10^{-7} \text{ H/m}$$

$$\omega_0 = \gamma(H_0 - M_0)$$

$$\omega_m = \gamma \times (4\pi M).$$

For large-signal applications, however, the higher order terms of m of h cannot be neglected. To obtain an exact solution for the two-signal case, all higher order harmonics through third order should be included.

$$\begin{aligned} m_r = {} & a_0 + a_1 \sin \omega_1 t + a_2 \cos \omega_1 t + a_3 \sin \omega_2 t + a_4 \cos \omega_2 t \\ & + a_5 \sin 2\omega_1 t + a_6 \cos 2\omega_1 t + a_7 \sin 2\omega_2 t \\ & + a_8 \cos 2\omega_2 t + a_9 \sin (\omega_1 + \omega_2)t \\ & + a_{10} \cos (\omega_1 + \omega_2)t + a_{11} \sin (\omega_1 - \omega_2)t \\ & + a_{12} \cos (\omega_1 - \omega_2)t + a_{13} \sin (3\omega_1 t) \\ & + a_{14} \cos (3\omega_1 t) + a_{15} \sin (3\omega_2 t) + a_{16} \cos (3\omega_2 t) \\ & + a_{17} \sin (2\omega_1 + \omega_2)t + a_{18} \cos (2\omega_1 + \omega_2)t \\ & + a_{19} \sin (2\omega_1 - \omega_2)t + a_{20} \cos (2\omega_1 - w_2)t \\ & + a_{21} \sin (\omega_1 + 2\omega_2)t + a_{22} \cos (\omega_1 + 2\omega_2)t \\ & + a_{23} \sin (\omega_1 - 2\omega_2)t + a_{24} \cos (\omega_1 - 2\omega_2)t \end{aligned} \tag{8a}$$

$$\begin{aligned} m_\theta = {} & b_0 + b_1 \sin \omega_1 t + b_2 \cos \omega_1 t + b_3 \sin \omega_2 t + b_4 \cos \omega_2 t \\ & + b_5 \sin 2\omega_1 t + b_6 \cos 2\omega_1 t + b_7 \sin 2\omega_2 t + b_8 \cos 2\omega_2 t \\ & + b_9 \sin (\omega_1 + \omega_2)t + b_{10} \cos (\omega_1 + \omega_2)t \\ & + b_{11} \sin (\omega_1 - \omega_2)t + b_{12} \cos (\omega_1 - \omega_2)t \\ & + b_{13} \sin (3\omega_1 t) + b_{14} \cos (3\omega_1 t) + b_{15} \sin (3\omega_2 t) \\ & + b_{16} \cos (3\omega_2 t) + b_{17} \sin (2\omega_1 + \omega_2)t \\ & + b_{18} \cos (2\omega_1 + \omega_2)t + b_{19} \sin (2\omega_1 - \omega_2)t \\ & + b_{20} \cos (2\omega_1 - \omega_2)t + b_{21} \sin (\omega_1 + 2\omega_2)t \\ & + b_{22} \cos (\omega_1 + 2\omega_2)t + b_{23} \sin (\omega_1 - 2\omega_2)t \\ & + b_{24} \cos (\omega_1 - 2\omega_2)t \end{aligned} \tag{8b}$$

$$\begin{aligned} m_z = {} & c_0 + c_1 \sin \omega_1 t + c_2 \cos \omega_1 t + c_3 \sin \omega_2 t + c_4 \cos \omega_2 t \\ & + c_5 \sin 2\omega_1 t + c_6 \cos 2\omega_1 t + c_7 \sin 2\omega_2 t \\ & + c_8 \cos 2\omega_2 t + c_9 \sin (\omega_1 + \omega_2)t + c_{10} \cos (\omega_1 + w_2)t \\ & + c_{11} \sin (\omega_1 - \omega_2)t + c_{12} \cos (\omega_1 - \omega_2)t \\ & + c_{13} \sin (3\omega_1 t) + c_{14} \cos (3\omega_1 t) + c_{15} \sin (3\omega_2 t) \\ & + c_{16} \cos (3\omega_2 t) + c_{17} \sin (2\omega_1 + \omega_2)t \\ & + c_{18} \cos (2\omega_1 + \omega_2)t + c_{19} \sin (2\omega_1 - \omega_2)t \\ & + c_{20} \cos (2\omega_1 - \omega_2)t + c_{21} \sin (\omega_1 + 2\omega_2)t \\ & + c_{22} \cos (\omega_1 + 2\omega_2)t + c_{23} \sin (\omega_1 - 2\omega_2)t \\ & + c_{24} \cos (\omega_1 - 2\omega_2)t. \end{aligned} \tag{8c}$$

There are 75 unknowns in (8a)–(8c) with each unknown corresponding to the magnitude of a specific harmonic. Seventy-five simultaneous equations are found by substituting (8a)–(8c) into the nonlinear equation of motion. Numerical techniques are necessary to solve these sets of equations. Since only the third-order intermodulation with frequencies $(2\omega_1 - \omega_2)$ and $(2\omega_2 - \omega_1)$ are of primary interest, it is unnecessary to solve the complete spectrum. In this paper, approximate solutions using an iterative process are derived. These analytical results are shown to approximate the experimental results obtained.

The two RF signals are denoted by the fields

$$h_r = h_{r1} \cos \omega_1 t + h_{r2} \cos \omega_2 t + h_{r3} \sin \omega_1 t + h_{r4} \sin \omega_2 t \tag{9}$$

$$h_\theta = h_{\theta 1} \cos \omega_1 t + h_{\theta 2} \cos \omega_2 t + h_{\theta 3} \sin \omega_1 t + h_{\theta 4} \sin \omega_2 t. \tag{10}$$

As indicated, h_{r3},h_{r4} are in quadrature phase with respect to h_{r1},h_{r2}, respectively. Similarly, $h_{\theta 3}$,$h_{\theta 4}$ are in quadrature phase with respect to $h_{\theta 1}$,$h_{\theta 2}$, respectively.

The unknown RF magnetization, which consists of only the fundamental frequencies ω_1,ω_2, and the intermodulation frequency $(2\omega_1 - \omega_2)$ are given by

$$m_r = m_{r1}\cos\omega_1 t + m_{r2}\cos\omega_2 t + m_{r3}\sin\omega_1 t + m_{r4}\sin\omega_2 t \tag{11a}$$

$$m_\theta = m_{\theta1}\cos\omega_1 t + m_{\theta2}\cos\omega_2 t + m_{\theta3}\sin\omega_1 t + m_{\theta4}\sin\omega_2 t + m_{\theta5}\cos(2\omega_1 - \omega_2)t + m_{\theta6}\sin(2\omega_1 - \omega_2)t \tag{11b}$$

$$m_z = m_{z1}\cos 2\omega_1 t + m_{z2}\cos 2\omega_2 t + m_{z3}\cos(\omega_1 + \omega_2)t + m_{z4}\cos(\omega_1 - \omega_2)t + m_{z5}\sin(2\omega_1 t) + m_{z6}\sin(2\omega_2 t) + m_{z7}\sin(\omega_1 + \omega_2)t + m_{z8}\sin(\omega_1 - \omega_2)t. \tag{11c}$$

It should be observed that the intermodulation components of m_r are neglected because only the m_θ component is strongly coupled to the output transmission lines in a distributed-type circulator. This will be further explained in the next section. In addition, only the second-order harmonic terms are included in m_z. This is because [as indicated in (6)] second-order terms are the lowest order in the m_z component. It is through these second-order harmonic terms that the third-order intermodulation product is produced.

Substituting (9), (10), (11a), (11b) into (4) and (5) and neglecting the $m_{\theta5},m_{\theta6}$ terms for the time being, the following solutions for m_r,m_θ are found by comparing the coefficients at both sides of the equal sign. The first-order solutions m_r,m_θ are found to be

$$m_{r1} = \frac{\gamma^2(H_0 - M_0)M_0h_{r1} - \gamma M_0\omega_1 h_{\theta3}}{\gamma^2(H_0 - M_0)^2 - \omega_1^2} \tag{12a}$$

$$m_{r2} = \frac{\gamma^2(H_0 - M_0)M_0h_{r2} - \gamma M_0\omega_2 h_{\theta4}}{\gamma^2(H_0 - M_0)^2 - \omega_2^2} \tag{12b}$$

$$m_{r3} = \frac{\gamma^2(H_0 - M_0)M_0h_{r3} + \gamma M_0\omega_1 h_{\theta1}}{\gamma^2(H_0 - M_0)^2 - \omega_1^2} \tag{12c}$$

$$m_{r4} = \frac{\gamma^2(H_0 - M_0)M_0h_{r4} + \gamma M_0\omega_0 h_{\theta2}}{\gamma^2(H_0 - M_0)^2 - \omega_2^2} \tag{12d}$$

$$m_{\theta1} = \frac{\gamma^2M_0(H_0 - M_0)h_{\theta1} + \gamma M_0\omega_1 h_{r3}}{\gamma^2(H_0 - M_0)^2 - \omega_1^2} \tag{13a}$$

$$m_{\theta2} = \frac{\gamma^2M_0(H_0 - M_0)h_{\theta2} + \gamma M_0\omega_2 h_{r4}}{\gamma^2(H_0 - M_0)^2 - \omega_2^2} \tag{13b}$$

$$m_{\theta3} = \frac{\gamma^2M_0(H_0 - M_0)h_{\theta3} - \gamma M_0\omega_1 h_{r1}}{\gamma^2(H_0 - M_0)^2 - \omega_1^2} \tag{13c}$$

$$m_{\theta4} = \frac{\gamma^2M_0(H_0 - M_0)h_{\theta4} - \gamma M_0\omega_2 h_{r2}}{\gamma^2(H_0 - M_0)^2 - \omega_2^2}. \tag{13d}$$

The following identities have been established from the small-signal theory [11]:

$$\frac{\gamma^2M_0(H_0 - M_0)}{\gamma^2(H_0 - M_0)^2 - \omega_1^2} = \mu_1 - 1 \tag{14a}$$

$$\frac{\gamma M_0\omega_1}{\gamma^2(H_0 - M_0)^2 - \omega_1^2} = \kappa_1 \tag{14b}$$

$$\frac{\gamma^2M_0(H_0 - M_0)}{\gamma^2(H_0 - M_0)^2 - \omega_2^2} = \mu_2 - 1 \tag{14c}$$

$$\frac{\gamma M_0\omega_2}{\gamma^2(H_0 - M_0)^2 - \omega_2^2} = \kappa_2 \tag{14d}$$

where μ and κ are the regular Polder tensor elements in small-signal theory. Using the notation of (14), one can simplify (12) and (13) to the following form:

$$m_{r1} = (\mu_1 - 1)h_{r1} - \kappa_1 h_{\theta3} \tag{15a}$$

$$m_{r2} = (\mu_2 - 1)h_{r2} - \kappa_2 h_{\theta4} \tag{15b}$$

$$m_{r3} = (\mu_1 - 1)h_{r3} + \kappa_1 h_{\theta1} \tag{15c}$$

$$m_{r4} = (\mu_2 - 1)h_{r4} + \kappa_2 h_{\theta2} \tag{15d}$$

$$m_{\theta1} = (\mu_1 - 1)h_{\theta1} + \kappa_1 h_{r3} \tag{16a}$$

$$m_{\theta2} = (\mu_2 - 1)h_{\theta2} + \kappa_2 h_{r4} \tag{16b}$$

$$m_{\theta3} = (\mu_1 - 1)h_{\theta3} - \kappa_1 h_{r1} \tag{16c}$$

$$m_{\theta4} = (\mu_2 - 1)h_{\theta4} - \kappa_2 h_{r2}. \tag{16d}$$

The preceding solutions are essentially the first-order solution which has been derived in the small-signal case. The m_z solution can be found by substituting the first-order solution back into (6). The second-order solutions for m_z are given by

$$m_{z1} = -\left(\frac{\gamma}{2}\right)\frac{(m_{r1}h_{\theta3} + m_{r3}h_{\theta1} - m_{\theta1}h_{r3} - m_{\theta3}h_{r1})}{2\omega_1} \tag{17a}$$

$$m_{z2} = -\left(\frac{\gamma}{2}\right)\frac{(m_{r2}h_{\theta4} + m_{r4}h_{\theta2} - m_{\theta2}h_{r4} - m_{\theta4}h_{r2})}{2\omega_2} \tag{17b}$$

$$m_{z3} = -\left(\frac{\gamma}{2}\right)\frac{(m_{r1}h_{\theta4} + m_{r2}h_{\theta3} + m_{r3}h_{\theta2} + m_{r4}h_{\theta1} - m_{\theta1}h_{r4} - m_{\theta2}h_{r3} - m_{\theta3}h_{r2} - m_{\theta4}h_{r1})}{(\omega_1 + \omega_2)} \tag{17c}$$

$$m_{z4} = -\left(\frac{\gamma}{2}\right)\frac{(-m_{r1}h_{\theta4} + m_{r2}h_{\theta3} + m_{r3}h_{\theta2} - m_{r4}h_{\theta1} + m_{\theta1}h_{r4} - m_{\theta2}h_{r3} - m_{\theta3}h_{r2} + m_{\theta4}h_{r1})}{(\omega_1 - \omega_2)} \tag{17d}$$

$$m_{z5} = \left(\frac{\gamma}{2}\right) \frac{(m_{r1}h_{\theta 1} - m_{r3}h_{\theta 3} - m_{\theta 1}h_{r1} + m_{\theta 3}h_{r3})}{2\omega_1} \tag{17e}$$

$$m_{z6} = \left(\frac{\gamma}{2}\right) \frac{(m_{r2}h_{\theta 2} - m_{r4}h_{\theta 4} - m_{\theta 2}h_{r2} + m_{\theta 4}h_{r4})}{2\omega_2} \tag{17f}$$

$$m_{z7} = \left(\frac{\gamma}{2}\right) \frac{(m_{r1}h_{\theta 2} + m_{r2}h_{\theta 1} - m_{r3}h_{\theta 4} - m_{r4}h_{\theta 3} - m_{\theta 1}h_{r2} - m_{\theta 2}h_{r1} + m_{\theta 3}h_{r4} + m_{\theta 4}h_{r3})}{(\omega_1 + \omega_2)} \tag{17g}$$

$$m_{z8} = \left(\frac{\gamma}{2}\right) \frac{(m_{r1}h_{\theta 2} + m_{r2}h_{\theta 1} + m_{r3}h_{\theta 4} + m_{r4}h_{\theta 3} - m_{\theta 1}h_{r2} - m_{\theta 2}h_{r1} - m_{\theta 3}h_{r4} - m_{\theta 4}h_{r3})}{(\omega_1 - \omega_2)}. \tag{17h}$$

The third-order intermodulation product can be found by substituting all of the first- and second-order solutions back into (4) and (5). By this iterative process, higher order solutions can be obtained. After the mathematical multiplication, many harmonic terms are generated. If only the intermodulation harmonic $(2\omega_1 - \omega_2)$ terms are collected, the magnetization terms for the $2\omega_1 - \omega_2$ frequency are given by

$$m_{\theta 5} = -\left(\frac{\gamma}{2}\right) \frac{(m_{z8}h_{r1} + m_{z5}h_{r2} + m_{z4}h_{r3} - m_{z1}h_{r4} + m_{z8}m_{r1} + m_{z5}m_{r2} + m_{z4}m_{r3} - m_{z1}m_{r4})}{(2\omega_1 - \omega_2)} \tag{18a}$$

$$m_{\theta 6} = \left(\frac{\gamma}{2}\right) \frac{(m_{z4}h_{r1} + m_{z1}h_{r2} - m_{z8}h_{r3} + m_{z5}h_{r4} + m_{z4}m_{r1} + m_{z1}m_{r2} - m_{z8}m_{r3} + m_{z5}m_{r4})}{(2\omega_1 - \omega_2)}. \tag{18b}$$

The preceding expressions are functions of both the fundamental and the second-order harmonics. More useful expressions which are functions of only the fundamental fields h_{r1}, $h_{\theta 1}$, h_{r2}, and $h_{\theta 2}$ can be derived by using (15)–(18). In terms only fundamental fields, the second-order terms are given by

$$m_{z1} = -\left(\frac{\gamma}{2}\right) \frac{\kappa_1(h_{r1}^2 + h_{\theta 1}^2 - h_{r3}^2 - h_{\theta 3}^2)}{2\omega_1} \tag{19a}$$

$$m_{z5} = -\left(\frac{\gamma}{2}\right) \frac{2\kappa_1(h_{r1}h_{r3} + h_{\theta 1}h_{\theta 3})}{2\omega_1} \tag{19b}$$

$$m_{z4} = -\left(\frac{\gamma}{2}\right) \frac{\left\{\begin{array}{l}(\mu_1 - \mu_2)(h_{r3}h_{\theta z} + h_{r4}h_{\theta 1} - h_{r1}h_{\theta 4} - h_{r2}h_{\theta 3}) \\ \quad + (\kappa_1 - \kappa_2)(h_{\theta 1}h_{\theta 2} + h_{\theta 3}h_{\theta 4} + h_{r1}h_{r2} + h_{r3}h_{r4})\end{array}\right\}}{(\omega_1 - \omega_2)} \tag{19c}$$

$$m_{z8} = \left(\frac{\gamma}{2}\right) \frac{\left\{\begin{array}{l}(\mu_1 - \mu_2)(h_{r1}h_{\theta 2} - h_{r2}h_{\theta 1} + h_{r3}h_{\theta 4} - h_{\theta 3}h_{r4}) \\ \quad + (\kappa_1 - \kappa_2)(h_{r1}h_{r4} + h_{\theta 1}h_{\theta 4} - h_{r2}h_{r3} - h_{\theta 2}h_{\theta 3})\end{array}\right\}}{(\omega_1 - \omega_2)}. \tag{19d}$$

In terms of only the fundamental fields, the third-order intermodulation magnetization terms are calculated to be

$$m_{\theta 5} = -\left(\frac{\gamma}{2}\right) \frac{\left\{\begin{array}{l}\left(\frac{\gamma\kappa_1}{2\omega_1}\right)\left[\frac{(\mu_2 h_{r4} + \kappa_2 h_{\theta 2})}{2}(h_{r1}^2 + h_{\theta 1}^2 - h_{r3}^2 - h_{\theta 3}^2) - (\mu_2 h_{r2} - \kappa_2 h_{\theta 4})(h_{r1}h_{r3} + h_{\theta 1}h_{\theta 3})\right] \\ \quad - \frac{\gamma(\mu_1 h_{r3} + \kappa_1 h_{\theta 1})}{2(\omega_1 - \omega_2)}\left[(\mu_1 - \mu_2)(h_{r3}h_{\theta 2} + h_{r4}h_{\theta 1} - h_{r1}h_{\theta 4} - h_{r2}h_{\theta 3}) + (\kappa_1 - \kappa_2)(h_{\theta 1}h_{\theta 2}\right. \\ \quad \left. + h_{\theta 3}h_{\theta 4} + h_{r1}h_{r2} + h_{r3}h_{r4})\right] + \frac{\gamma(\mu_1 h_{r1} - \kappa_1 h_{\theta 3})}{2(\omega_1 - \omega_2)}\left[(\mu_1 - \mu_2)(h_{r1}h_{\theta 2} - h_{r2}h_{\theta 1}\right. \\ \quad \left. + h_{r3}h_{\theta 4} - h_{\theta 3}h_{r4}) + (\kappa_1 - \kappa_2)(h_{r1}h_{r4} + h_{\theta 1}h_{\theta 4} - h_{r2}h_{r3} - h_{\theta 2}h_{\theta 3})\right]\end{array}\right\}}{(2\omega_1 - \omega_2)} \tag{20a}$$

$$m_{\theta 6} = -\left(\frac{\gamma}{2}\right) \frac{\left\{ \begin{array}{l} \frac{\gamma\kappa_1}{4\omega_1}(\mu_2 h_{r2} - \kappa_2 h_{\theta 4})(h_{r1}^2 + h_{\theta 1}^2 - h_{r3}^2 - h_{\theta 3}^2) + \frac{\gamma\kappa_1}{2\omega_1}(h_{r1}h_{r3} + h_{\theta 1}h_{\theta 3})(\mu_2 h_{r4} + \kappa_2 h_{\theta 2}) \\ + \frac{\gamma(\mu_1 h_{r1} - \kappa_1 h_{\theta 3})}{2(\omega_1 - \omega_2)}[(\mu_1 - \mu_2)(h_{r3}h_{\theta 2} + h_{r4}h_{\theta 1} - h_{r1}h_{\theta 4} - h_{r2}h_{\theta 3}) + (\kappa_1 - \kappa_2)(h_{\theta 1}h_{\theta 2} \\ + h_{\theta 3}h_{\theta 4} + h_{r1}h_{r2} + h_{r3}h_{r4})] + \frac{\gamma(\mu_1 h_{r3} + \kappa_1 h_{\theta 1})}{2(\omega_1 - \omega_2)}[(\mu_1 - \mu_2)(h_{r1}h_{\theta 2} - h_{r2}h_{\theta 1} \\ + h_{r3}h_{\theta 4} - h_{\theta 3}h_{r4}) + (\kappa_1 - \kappa_2)(h_{r1}h_{r4} + h_{\theta 1}h_{\theta 4} - h_{r2}h_{r3} - h_{\theta 2}h_{\theta 3})] \end{array} \right\}}{(2\omega_1 - \omega_2)}. \quad (20b)$$

The preceding two expressions indicate the third-order intermodulation magnetizations $m_{\theta 5}$ and $m_{\theta 6}$ in terms of the known fundamental fields h_{r1}, h_{r2}, h_{r3}, h_{r4}, $h_{\theta 1}$, $h_{\theta 2}$, $h_{\theta 3}$, and $h_{\theta 4}$. The μ_1,κ_1, and μ_2,κ_2 are Polder tensor elements for the ferrite material at frequencies ω_1 and ω_2, respectively.

It should be noted that in the expressions for intermodulation, the intermodulation magnetization $m_{\theta 5}$ and $m_{\theta 6}$ are proportional to the off-diagonal Polder tensor element κ, which is the principal factor in ferrite characteristics. In the case of a pure dielectric medium ($\mu_1 = \mu_2 = 1$ and $\kappa_1 = \kappa_2 = 0$), both of the preceding intermodulation terms vanish. This means that in an ideally linear dielectric material, no intermodulation distortion can occur. The main cause of intermodulation distortion in ferrite materials is due to the κ factor.

It should also be noted that the intermodulation magnetization ($m_{\theta 5}$,$m_{\theta 6}$) derived here gives only the magnetic dipole moment (which can be a source for electromagnetic fields) produced by the fundamental signal. In other words, these terms give the magnetic dipole moment oscillating at the intermodulation frequency $(2\omega_1 - \omega_2)$ at a particular point in the ferrite medium, caused by the fundamental fields h_r and h_θ at that particular point. The actual amount of power at the intermodulation frequency $(2\omega_1 - \omega_2)$ depends heavily upon the condition of the coupling. If the coupling is weak, very little power at the intermodulation frequency is produced. On the other hand, a large amount of power can be generated if the coupling is very strong. In a distributed-type circulator, the coupling between the field and the magnetization is through the circular ferrite disk resonator. In the next section, a calculation of the coupling between intermodulation fields and the magnetization source is presented. Once the fundamental fields h_r and h_θ for frequencies ω_1 and ω_2 are known, (20a) and (20b) can be applied to estimate intermodulation for arbitrary coupling structure.

Finally, the complete expression for the magnetization of the intermodulation signal is given by

$$m_\theta = m_{\theta 5} \cos(2\omega_1 - \omega_2)t + m_{\theta 6} \sin(2\omega_1 - \omega_2)t \quad (21)$$

where $m_{\theta 5}$ and $m_{\theta 6}$ are given by (20a) and (20b).

III. COUPLING OF THE INTERMODULATION SIGNAL TO THE OUTPUT TRANSMISSION LINES IN A DISTRIBUTED CIRCULATOR

The theory of a distributed-type circulator has been developed by Bosma [12] and Fay and Comstock [13]. The complete theory of circulators requires the use of the Green's function which is very complicated. A brief description of the circulator will be given here. Fig. 1 shows the structure of a typical distributed-type circulator. Three transmission lines, either stripline or microstrip, are connected to a circular conducting disk. The choice of a magnetic wall at $r = R$ as the boundary condition requires that only the TM_{011} mode is resonant. Fig. 1(a) shows the mode pattern before the ferrite is magnetized. With an input power at port 1, a resonant TM_{011} field pattern is induced as shown in Fig. 1(a) (solid lines representing the magnetic field). Note that points A and B are two null points in this field pattern and no signal is present at these two nulls. In Fig. 1(a), an equal amount of input power is transmitted to port 2 and to port 3 with a small

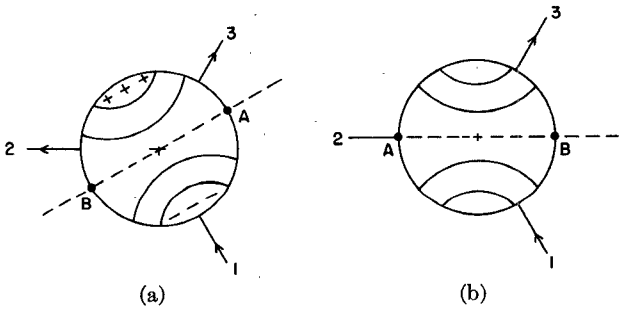

Fig. 1. TM_{011} mode field pattern inside a circulator before (a) and after (b) the magnetic field is applied.

amount of reflection at the input. However, when the ferrite is biased with a proper dc magnetic field, the TM_{011} mode pattern is rotated to a new position where one of the nulls (point A) moves to the isolated port 2. Since there is no energy at the null, port 2 is isolated and all the input power is transmitted to the output port 3. This pattern rotation theory has been derived experimentally by Fay and Comstock [13] and proved theoretically by Wu and Rosenbaum [14].

The goal of this section is to determine the coupling between the circulator and the intermodulation magnetization; i.e., how much intermodulation is produced by those magnetic dipoles which are generated by the large fundamental signal fields. Fig. 2 shows the distributed-type circulator with input at port 1 and output at port 2. The ω_1 signal is sent in through port 1 and the ω_2 signals sent in through port 2 (output). The third port is terminated as usual. Only the case where the interference signal ω_2 comes in through the output port is considered.

Since the frequency $(2\omega_1 - \omega_2)$ of the strong third-order intermodulation noise is very close to the main signal frequency ω_1 which is resonant in the TM_{011} mode in the disk, the intermodulation field is also resonant in the TM_{011} mode. A special property of the TM_{011} mode is that its electric field E_z vanishes at the center because the Bessel function of the first kind $J_1(kr)$ vanishes at $r = 0$ [15]. A line integral for electric field E_z can be taken along the rectangle shown by the dotted line in Fig. 2 going through the top conductor, the edge, the bottom conductor, and the disk center. Because the electric field must vanish at the conducting boundary, $E_1 = E_3 = 0$, and since $E_2 = 0$ at the center (as explained before), the only contribution to this line integral comes from the electric field at the disk edge.

Using the Maxwell equation [16]

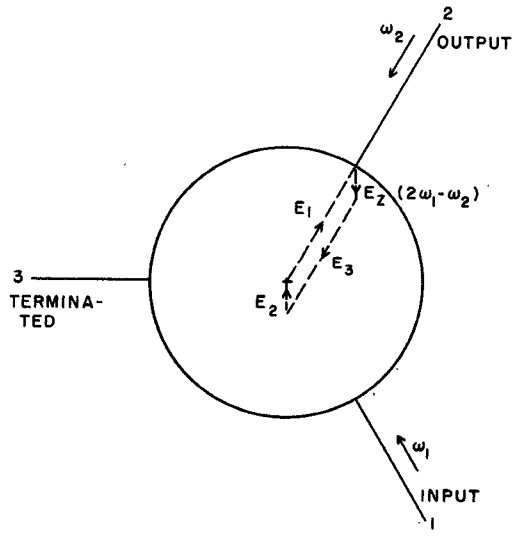

Fig. 2. Rectangular loop showing the coupling between field and magnetization for an intermodulation signal in a circulator.

$$\oint \boldsymbol{E}\cdot d\boldsymbol{l} = \frac{d}{dt}\iint \boldsymbol{B}_\theta \cdot d\boldsymbol{A} \tag{22}$$

where

$$\boldsymbol{B}_\theta = \mu_0 \boldsymbol{m}_\theta + \boldsymbol{h}_\theta = \mu_0 \boldsymbol{m}_\theta. \tag{23}$$

The reason only the m_θ terms were calculated in the last section is now obvious. Substitution of (21) into (22) gives the following expression for the electric field E_z at the output port:

$$E_{z(2\omega_1-\omega_2)} = \mu_0(2\omega_1 - \omega_2)\left[\sin(2\omega_1 - \omega_2)t \int_0^R m_{\theta 5}\, dr - \cos(2\omega_1 - \omega_2)t \int_0^R m_{\theta 6}\, dr\right]. \tag{24}$$

Before (20) for m_θ can be applied to calculate the intermodulation field, the field distribution of ω_1 and ω_2 must be known. Referring to Bosma's results [12], one has the field distribution for the ω_1 signal coming in through port 1 as

$$E_{z\omega_1} = \frac{\sqrt{3}}{2} A J_1(k_1 r)\sin\omega_1 t \tag{25a}$$

$$h_{r\omega_1} = -\left(\frac{A}{Z_{\text{eff}_1}}\right)\left(\frac{\sqrt{3}}{2}\right)\frac{\kappa_1}{\mu_1} J_1'(k_1 r)\sin\omega_1 t - \left(\frac{A}{Z_{\text{eff}_1}}\right)\left(\frac{1}{2}\right)\frac{J_1(k_1 r)}{(k_1 r)}\cos\omega_1 t \tag{25b}$$

$$h_{\theta\omega_1} = -\left(\frac{A}{Z_{\text{eff}_1}}\right)\left(\frac{1}{2}\right)\frac{\kappa_1}{\mu_1}\frac{J_1(k_1 r)}{(k_1 r)}\sin\omega_1 t + \left(\frac{A}{Z_{\text{eff}_1}}\right)\left(\frac{\sqrt{3}}{2}\right) J_1'(k_1 r)\cos\omega_1 t \tag{25c}$$

where

$$k_1 = \frac{\omega_1}{C}(\mu_{\text{eff}_1}\epsilon_f)^{1/2}$$

= radial wave propagation constant;

$$Z_{\text{eff}_1} = \eta(\mu_{\text{eff}_1}/\epsilon_f)^{1/2}$$

= effective impedance of ferrite at frequency ω_1;

$$\mu_{\text{eff}_1} = \frac{\mu_1^2 - \kappa_1^2}{\mu_1}$$

= effective permeability of ferrite at ω_1;

ϵ_f = relative dielectric constant of ferrite;

$\eta = 120\pi\Omega$ = intrinsic impedance of free space;

$C = 3 \times 10^8$ m/s = speed of light in vacuum.

The field distribution for the interfering signal ω_2 coming in through the output port 3, is given by

$$E_{z\omega_2} = -\frac{\sqrt{3}}{2} BJ_1(k_2 r) \sin \omega_2 t \tag{26a}$$

$$h_{r\omega_2} = \left(\frac{B}{Z_{\text{eff}_2}}\right)\left(\frac{\sqrt{3}}{2}\right)\frac{\kappa}{\mu_2} J_1'(k_2 r) \sin \omega_2 t - \left(\frac{B}{Z_{\text{eff}_2}}\right)\left(\frac{1}{2}\right)\frac{J_1(k_2 r)}{(k_2 r)} \cos \omega_2 t \tag{26b}$$

$$h_{\theta\omega_2} = -\left(\frac{B}{Z_{\text{eff}_2}}\right)\left(\frac{1}{2}\right)\frac{\kappa_2}{\mu_2}\frac{J_1(k_2 r)}{(k_2 r)} \sin \omega_2 t - \left(\frac{B}{Z_{\text{eff}_2}}\right)\left(\frac{\sqrt{3}}{2}\right) J_1'(k_2 r) \cos \omega_2 t \tag{26c}$$

where the variables are similar to those in (25) except that the subscripts are now for ω_2. The sign difference in (26c) is due to the different entry port.

From (25) and (26), all the fundamental components at frequencies ω_1 and ω_2 inside the circulator are known and are given by

$$h_{r1} = -\left(\frac{A}{Z_{\text{eff}_1}}\right)\left(\frac{1}{2}\right)\frac{J_1(k_1 r)}{(k_1 r)} \tag{27a}$$

$$h_{r2} = -\left(\frac{B}{Z_{\text{eff}_2}}\right)\left(\frac{1}{2}\right)\frac{J_1(k_2 r)}{(k_2 r)} \tag{27b}$$

$$h_{r3} = -\left(\frac{A}{Z_{\text{eff}_1}}\right)\left(\frac{\sqrt{3}}{2}\right)\frac{\kappa_1}{\mu_1} J_1'(k_1 r) \tag{27c}$$

$$h_{r4} = \left(\frac{B}{Z_{\text{eff}_2}}\right)\left(\frac{\sqrt{3}}{2}\right)\frac{\kappa_2}{\mu_2} J_1'(k_2 r) \tag{27d}$$

$$h_{\theta 1} = \left(\frac{A}{Z_{\text{eff}_1}}\right)\left(\frac{\sqrt{3}}{2}\right) J_1'(k_1 r) \tag{27e}$$

$$h_{\theta 2} = -\left(\frac{B}{Z_{\text{eff}_2}}\right)\left(\frac{\sqrt{3}}{2}\right) J_1'(k_2 r) \tag{27f}$$

$$h_{\theta 3} = -\left(\frac{A}{Z_{\text{eff}_1}}\right)\left(\frac{1}{2}\right)\left(\frac{\kappa_1}{\mu_1}\right)\left(\frac{J_1(k_1 r)}{(k_1 r)}\right) \tag{27g}$$

$$h_{\theta 4} = -\left(\frac{B}{Z_{\text{eff}_2}}\right)\left(\frac{1}{2}\right)\left(\frac{\kappa_2}{\mu_2}\right)\left(\frac{J_1(k_2 r)}{(k_2 r)}\right). \tag{27h}$$

Substituting (20) and (27) into (24), one can calculate the induced electric field for the intermodulation frequency $(2\omega_1 - \omega_2)$. Once the electric field is known, the power at the $(2\omega_1 - \omega_2)$ frequency can be calculated. For this calculation, the following four integrals involving Bessel functions are needed:

$$\alpha = \int_0^{x_{1.1}} \left[\frac{J_1(x)}{x}\right]^3 dx = 0.1588 \tag{28a}$$

$$\beta = \int_0^{x_{1.1}} \left[\frac{J_1(x)}{x}\right]^2 J_1'(x)\, dx = 0.1251 \tag{28b}$$

$$\lambda = \int_0^{x_{1.1}} \left[\frac{J_1(x)}{x}\right] [J_1'(x)]^2 dx = 0.1078 \tag{28c}$$

$$\delta = \int_0^{x_{1.1}} [J_1'(x)]^3 dx = 0.0964 \tag{28d}$$

where $x_{1.1} = 1.84$ and $k = (\omega/c)(\mu_{\text{eff}}\epsilon_f)^{1/2} \cong k_1 \cong k_2$.

An exact solution for these integrals appears to be infeasible. Hence the integrals are evaluated using numerical techniques and the results are presented in (28a)–(28d).

After considerable mathematical manipulations, the final results can be expressed as

$$(2\omega_1 - \omega_2)\int_0^R m_{\theta 5}\, dr = \frac{\sqrt{3}\gamma^2}{16(\omega_1 - \omega_2)k}\left(\frac{A^2 B}{Z_{\text{eff}_1}^2 Z_{\text{eff}_2}}\right)\mu_{\text{eff}_1}(\mu_{\text{eff}_1} - \mu_{\text{eff}_2})\beta \tag{29a}$$

$$(2\omega_1 - \omega_2)\int_0^\gamma m_{\theta 6}\, dr = \left(\frac{\gamma^2}{32k}\right)\left(\frac{A^2 B}{Z_{\text{eff}_1}^2 Z_{\text{eff}_2}}\right)\mu_{\text{eff}_1}\left[\left(\frac{\mu_{\text{eff}_2}}{\omega_1}\right)\left(\frac{\kappa_1}{\mu_1}\right)(3\lambda + \alpha) + \frac{[\mu_{\text{eff}_1}(\kappa_2/\mu_2) - \mu_{\text{eff}_2}(\kappa_1/\mu_1)]}{(\omega_1 - \omega_2)}(3\lambda - \alpha)\right]. \tag{29b}$$

At the output, the electric field E_z of the strong third-order intermodulation frequency $2\omega_1 - \omega_2$ is found to be

$$E_{z_{2\omega_1-\omega_2}} = \frac{\sqrt{3}\mu_0\gamma^2}{16(\omega_1 - \omega_2)k}\left(\frac{A^2 B}{Z_{\text{eff}_1}^2 Z_{\text{eff}_2}}\right) \cdot \mu_{\text{eff}_1}(\mu_{\text{eff}_1} - \mu_{\text{eff}_2})\beta \sin(2\omega_1 - \omega_2)t - \left(\frac{\gamma^2\mu_0}{32k}\right)\left(\frac{A^2 B}{Z_{\text{eff}_1}^2 Z_{\text{eff}_2}}\right)\mu_{\text{eff}_1}\left[\left(\frac{\mu_{\text{eff}_2}}{\omega_1}\right)\left(\frac{\kappa_1}{\mu_1}\right)(3\lambda + \alpha) + \frac{[\mu_{\text{eff}_1}(\kappa_2/\mu_2) - \mu_{\text{eff}_2}(\kappa_1/\mu_1)]}{(\omega_1 - \omega_2)}(3\lambda - \alpha)\right] \cdot \cos(2\omega_1 - \omega_2)t. \tag{30}$$

The intermodulation noise is found to follow the power series law for the third-order approximation. In addition, the electric field is proportional to the value of κ's and inversely proportional to the cube of the effective intrinsic impedance. In the next section, an example is given to compare the estimated intermodulation power level with the fundamental power levels.

IV. EXAMPLES

The amount of third-order intermodulation that will be produced in a distributed-type circulator operating at VHF frequencies is calculated in this section. Consider a VHF distributed-type circulator with the following characteristics:

1) saturation magnetization of ferrite, $4\pi M_s = 600$ G,
2) dc bias magnetic field, $H_0 = 800$ Oe;
3) relative dielectric constant of ferrite, $\epsilon_f = 16$;
4) main signal frequency is 125 MHz;
5) interfering signal frequency is 130 MHz.

From these assumed parameters, the following device parameters can be calculated:

$$f_0 = \gamma(H_0 - M_0) = 0.56 \times 10^9 \text{ s}^{-1}$$

$$f_m = \gamma \times 4\pi M_s = 1.68 \times 10^9 \text{ s}^{-1}$$

$$\mu_1 = 4.157312$$

$$\mu_2 = 4.170880$$

$$\kappa_1 = 0.704757$$

$$\kappa_2 = 0.739508$$

$$\mu_{\text{eff}_1} = 4.03808$$

$$\mu_{\text{eff}_2} = 4.03976$$

$$Z_{\text{eff}_1} = Z_{\text{eff}_2} = 188\ \Omega.$$

For this example, the power level of the main signal (f_1) is assumed to be 1 W ($P_{f_1} = +30$ dBm) and the power level of the interfering signal (f_2) is 20 dB down or $P_{f_2} =$ 10 dBm. From this information and an assumed 1-cm^2 input-port cross-sectional area, one has

$$A = 10^3 \text{ V/m}$$

$$B = 10^2 \text{ V/m}.$$

The electric field strength for the intermodulation signal can be calculated from (30)

$$E_{z_{2\omega_1-\omega_2}} \simeq 0.205 \times 10^{-4} \sin(2\omega_1 - \omega_2)t + 2.43 \times 10^{-4} \cos(2\omega_1 - \omega_2)t.$$

The absolute value of $E_{z2\omega_1-\omega_2}$ is approximately $|E_{z1}| \simeq 2.43 \times 10^{-4}$ V/m. The power ratio of the intermodulation signal to the fundamental ω_1 signal is given by

$$\frac{P_{2f_1-f_2}}{P_{f_1}} = \left[\frac{E_{z_{2\omega_1-\omega_2}}}{E_{z\omega_1}}\right]^2 = 5.9 \times 10^{-14}.$$

Therefore, at fundamental power levels $P_{f_1} = 30$ dBm, $P_{f_2} = 10$ dBm, the estimated intermodulation power level is

$$P_{2f_1-f_2} = -102 \text{ dBm}.$$

The intermodulation power level is 132 dB down from the strong fundamental power P_{f_1} (when $P_{f_1} = +30$ dBm) for the distributed-type circulator in this example. Since the third-order intermodulation product in a distributed circulator follows the power series rule, the intermodulation power level will increase to $P_{2f_1-f_2} = -42$ dBm for a main signal power of $P_{f_1} = 100$ W (50 dBm) and an interfering signal power of $P_{f_2} = 1$ W (30 dBm). Thus the calculated intermodulation term is approximately 92 dB down from P_{f_1}.

An experimental distributed VHF circulator recently built by Addington Laboratories has been tested for intermodulation performance. For a main signal power of $P_{f_1} = 50$ W (47 dBm) and an interfering signal power of $P_{f_2} = 0.5$ W (27 dBm), the measured third-order intermodulation at $2f_1 - f_2$ is -39 dBm from $f_1 = 122$ MHz and $f_2 = 126$ MHz. For the same power levels but for $f_1 = 126$ MHz and $f_2 = 134$ MHz, the measured third-order intermodulation at $2f_1 - f_2$ is -44 dBm. For the latter case, if P_{f_1} is increased to 75 W (48.5 dBm) and P_{f_2} is 0.75 W (28.5 dBm), the strong third-order intermodulation is measured to be -42 dBm.

Thus, for this experimental distributed circulator operating at the specified power levels, the dominating intermodulation term is approximately 86–91 dB down from P_{f_1}. Several other VHF and UHF distributed circulators have also been tested. Experimental results indicate that the intermodulation product is in the range of 80–100 dB down from the main signal when P_{f_1} is 50–100 W and P_{f_2} is 20 dB down from P_{f_1}.

V. CONCLUSIONS

An iterative process is used to calculate the third-order nonlinearity in ferrites. This nonlinearity is coupled by the circulator disk resonator to the outside transmission line to produce the third-order intermodulation terms. Analytic expressions are obtained for the field strength and power level of the intermodulation signal. It is found that the field strength of the intermodulation signal is proportional to the off-diagonal Polder tensor element κ and inversely proportional to the cube of the intrinsic effective wave impedance Z_{eff} of the ferrite material.

From this theoretical study, a low-intermodulation noise circulator can be achieved by choosing low-magnetization and high-wave-impedance ferrite material. However, a lower magnetization can be obtained only at the expense of bandwidth. Therefore a compromise between the bandwidth and intermodulation power level should be considered in the design of a circulator. From the analytic expression for $E_{z2f_1-f_2}$, the intermodulation level appears not to be a strong function of the frequency difference, $\omega_1 - \omega_2$. This is mainly due to the slow variation of effective permeability μ_{eff} with respect to frequency. Since the field strength of the intermodulation signal is proportional to the square of the f_1 field and directly proportional to the f_2 field strength, the power series rule is followed by the intermodulation noise produced in a distributed-type circulator.

Because the volume of the distributed-type circulator is normally larger than that of the lumped-element circulator [17], [18], the field strength in the distributed-type circulator is smaller than that of the lumped counterpart. Therefore the intermodulation noise produced in a distributed-type circulator will in general be less than that produced in a lumped-element circulator.

ACKNOWLEDGMENT

The authors wish to thank L. Bosin of Systems Research and Development Branch, Federal Aviation Administration, for helpful discussions and support.

REFERENCES

[1] W. P. Ayres, P. H. Vartanian, and J. L. Melchor, "Frequency doubling in ferrites," *J. Appl. Phys.*, vol. 27, pp. 188–189, Feb. 1956.
[2] J. E. Pippin, "Frequency doubling and mixing in ferrites," Gordon McKay Lab., Harvard Univ., Cambridge, MA, Sci. Rep. 2, AFCRL-TN-56-369, May 5, 1956.
[3] J. L. Melchor, W. P. Ayres, and P. H. Vartanian, "Microwave frequency doubling from 9 to 18 KMC in ferrites," *Proc. IRE*, vol. 45, pp. 643–646, May 1957.
[4] R. L. Jepsen, "Harmonic generation and frequency mixing in ferromagnetic insulators," *J. Appl. Phys.*, vol. 32, pp. 2627–2630, Dec. 1961.
[5] R. T. Denton, "A ferromagnetic amplifier using longitudinal pumping," *Proc. IRE* (Corresp.), vol. 48, pp. 937–938, May 1960.
[6] H. Suhl, "Theory of the ferromagnetic microwave amplifier," *J. Appl. Phys.*, vol. 28, pp. 1225–1236, Nov. 1957.
[7] M. T. Weiss, "A solid-state microwave amplifier and oscillator using ferrites," *Phys. Rev.*, vol. 107, p. 317, July 1957.
[8] H. Suhl, "The nonlinear behavior of ferrites at high microwave signal levels," *Proc. IRE*, vol. 44, pp. 1270–1284, Oct. 1956.
[9] L. Landau and E. Lifschitz, "On the theory of the dispersion of magnetic permeability in ferromagnetic bodies," *Phys. Z. Sowjetunion*, vol. 8, p. 153, 1935.
[10] D. Polder, "On the theory of ferromagnetic resonance," *Phil. Mag.*, vol. 40, pp. 99–115, Jan. 1949.
[11] J. Helszajn, *Principles of Microwave Ferrite Engineering*. New York: Wiley-Interscience, 1969.
[12] H. Bosma, "On stripline *Y*-circulation at UHF," *IEEE Trans. Microwave Theory Tech.* (*1963 Symposium Issue*), vol. MTT-12, pp. 61–72, Jan. 1964.
[13] C. E. Fay and R. L. Comstock, "Operation of the ferrite junction circulator," *IEEE Trans. Microwave Theory Tech.* (*1964 Symposium Issue*), vol. MTT-13, pp. 15–27, Jan. 1965.
[14] Y. S. Wu and F. J. Rosenbaum, "Wide-band operation of microstrip circulators," *IEEE Trans. Microwave Theory Tech.*, vol. MTT-22, pp. 849–856, Oct. 1974.
[15] M. Abramoritz and I. A. Segun, *Handbook of Mathematical Functions*. New York: Dover, 1965.
[16] R. E. Collins, *Foundations of Microwave Engineering*. New York: McGraw-Hill, 1966.
[17] Y. Konishi, "Lumped element *Y* circulator" *IEEE Trans. Microwave Theory Tech.* (*1965 Symposium Issue*), vol. MTT-13, pp. 852–864, Nov. 1965.
[18] Y. Konishi, "A high-power UHF circulator," *IEEE Trans. Microwave Theory Tech.* (*1967 Symposium Issue*), vol. MTT-15, pp. 700–708, Dec. 1967.

A Theoretical Study of Light Beams Guided Along Tapered Lenslike Media, and Their Applications

SHINNOSUKE SAWA, MEMBER, IEEE

***Abstract*—Propagation behavior of light beams along the tapered lenslike media, in which both the focusing parameter and the on-axis permittivity have gradients in the axial direction, is investigated in detail, theoretically and numerically, with the help of the approximate wave theory. As a result, it is clarified that the tapered lenslike media can be classified into two kinds, according to the differences of the focusing property. Matched incidence conditions to eliminate the fluctuations of the light beam are also clarified. As an application of the theory, a spot-size transducer and a mode transducer for use in a circular bend of the light focusing waveguide are proposed, and the design conditions are derived. A ray-oscillation suppressor (ROS) is also proposed, and its applicability to some new optical circuit components is discussed.**

Manuscript received April 7, 1975; revised August 7, 1975. This work was supported by the Science Research Fund of the Ministry of Education. Numerical calculations were done on FACOM 230-60 at the Data Processing Center, Kyoto University, and NEAC 2200-700•500 at the Computer Center, Osaka University.

The author is with the Department of Electronics, Faculty of Engineering, Ehime University, Matsuyama City, 790 Japan.

I. INTRODUCTION

OPTICAL waveguides such as parabolic-index fibers termed SELFOC [1] are technologically important because of the applicability to optical communication, optical instruments, and optical date processing. As is well known, waveguides of this type consist of a lens-like medium whose permittivity decreases quadratically with distance in the transverse direction from the guide axis.

The lenslike medium with a permittivity profile varying not only in the transverse direction but also in the direction of the guide axis may be termed a "tapered lenslike medium." The tapered lenslike medium is expected to have various interesting applications to optical circuit components, since it has a light-focusing property varying slowly and continuously along the axial direction.

Several papers have already been reported on the tapered lenslike media [2]–[6]. For example, Tien *et al.*